International Journal of Mineral Processing 98 (2011) 195–201

Contents lists available at ScienceDirect

International Journal of Mineral Processing

journal homepage: www.elsevier.com/locate/ijminpro

A thermogravimetric study of refractory clays chlorination

R.P. Orosco [a,b], E. Perino [b], M. del C. Ruiz [a,b,*], J.A. González [a,c]

[a] Instituto de Investigaciones en Tecnología Química-CONICET, INTEQUI, CC: 290-5700-San Luis, Argentina
[b] Facultad de Química, Bioquímica y Farmacia, Universidad Nacional de San Luis, Chacabuco y Pedernera, 5700-San Luis, Argentina
[c] Instituto de Ciencias Básicas, Universidad Nacional de Cuyo, 550-Mendoza, Argentina

ARTICLE INFO

Article history:
Received 9 June 2010
Received in revised form 18 November 2010
Accepted 10 December 2010
Available online 21 December 2010

Keywords:
Refractory clays
Thermogravimetry
Purification
Chlorination

ABSTRACT

The chlorine effect on different samples of refractory clays has been studied within a wide temperature interval. The isothermal and non isothermal calcination assays were carried out in currents of N_2 and a mixture of Cl_2/N_2 (1:1), using a thermogravimetric system designed in our laboratory and masses of approximately 300 mg. Isothermal assays were also performed with masses of 2 g, using a fixed bed reactor with horizontal dynamic flow. The initial samples of refractory clays and the residues resulting from thermal treatments were characterized by X-ray fluorescence (XRF), X-ray diffraction (XRD), scanning electron microscopy (SEM), electron probe microanalysis (EPMA), specific surface area analysis (BET) and CIELAB colorimetry.

The thermograms in N_2 and Cl_2/N_2 showed two mass losses, between room temperature and 650 °C, due to the elimination of the mineral hydration water and the transformation of kaolinite into metakaolinite. A third mass loss was observed over 750 °C in Cl_2/N_2 due to the chlorination and elimination of the iron contained in the samples. The X-ray diffractograms of the residues from the different thermal treatments showed that the calcination produced the total transformation of kaolinite and other phases contained in the mineral. The XRF analysis of the residues resulting from the isothermal assays in Cl_2/N_2 permitted to determine that the iron contained in the samples might be completely removed by chlorination at 900 °C for 2 h. The colorimetric analysis of the chlorination residues indicated that the discoloration and bleaching of samples were caused by the deferrification of the mineral. The results of the characterizations using SEM and EPMA supported the previous observations.

1. Introduction

Refractory clays are clays with an authigenic sedimentary origin, containing kaolinite as the main clay mineral constituent. These clays have a low content of iron, alkali and alkali earth cations. Refractory clays are found in nature together with other associated minerals and associated phases; thus, concentration and purification methods are needed for their industrial use (Bergaya et al., 2006). These processes are mainly physical such as washing, sieving, levigation, magnetic separation, etc. (Raghavan et al., 1997; Chandrasekhar and Ramaswamy, 2002; Maurya and Dixit, 1990). The physical methods are effective for certain contaminants, but they are insufficient for others, such as the iron, which determines the quality of these minerals. Most of the contaminating iron of clay is found finely dispersed among the mineral particles, generally as limonite, hydrohematites, goethite, amorphous hydrated oxide, hematite, magnetite, pyrite, etc. Also, iron is present in low proportion in the internal structure of the clay mineral. The elimination of iron from these minerals is difficult and expensive, and different methods are being investigated. Several authors such as Raghavan et al., 1997; Chandrasekhar and Ramaswamy, 2002, 2006, studied the High-gradientmagnetic separation (HGMS). These authors obtained iron extractions between 40 and 50%. The leaching with agents alone or together with reducing agents has also been reported (Veglio' and Toro, 1994; De Mesquita et al., 1996; Ambikadevi and Lalithambika, 2000; Atkinson and Fleming, 2001; Fabry and Kleindl, 2001).

The use of chlorination in the extractive metallurgy has greatly increased in the last decades (Jena and Brocchi, 1997) due to the progressive development of new chlorine-resistant materials, the simplicity of effluent control and the availability and variety of low cost chlorinating agents. The application of the chlorination processes to clays and kaolins has also been studied in order to use these minerals as aluminum source (Blumenthal and Wegner, 1989; Roder et al., 1987; Landsberg, 1975). The exhaust gases from chlorination cannot be emitted directly into the atmosphere; the gases must be scrubbed with NaOH solution to remove chlorine (Habashi, 1986, Vol 3). Although chlorine is a highly reactive chemical, it is possible to accomplish a safe use of this reagent by implementing appropriate security measures, in terms of storage and handling, to prevent potential leaks or spills. Moreover, simple

* Corresponding author. Instituto de Investigaciones en Tecnología Química-CONICET, INTEQUI, CC: 290-5700-San Luis, Argentina. Tel./fax: +54 2652 426711.
E-mail address: mruiz@unsl.edu.ar (M. del C. Ruiz).

0301-7516/$ – see front matter © 2010 Elsevier B.V. All rights reserved.
doi:10.1016/j.minpro.2010.12.004

Table 1
Chemical composition of the clay minerals used (%w/w).

Compound	APM112	AC1095	Timol
Al_2O_3	28	37	24
SiO_2	53	42	62
Fe_2O_3	3.5	0.8	1.2
$Na_2O + K_2O$	1.2	0.8	0.7
$CaO + MgO$	2.5	2.4	2.5

the chlorination of the different phases of iron oxides and hydroxides is not thermodynamically feasible up to temperatures higher than 1000 °C. However, although the partial pressure of the chlorinated species in equilibrium is very low, it is possible to remove iron chloride from the reaction zone when working in a flow system.

The efficacy of the chlorination process as an alternative method for the purification of clays has been demonstrated by González and Ruiz (2006). Using this methodology, the quantitative removal of iron

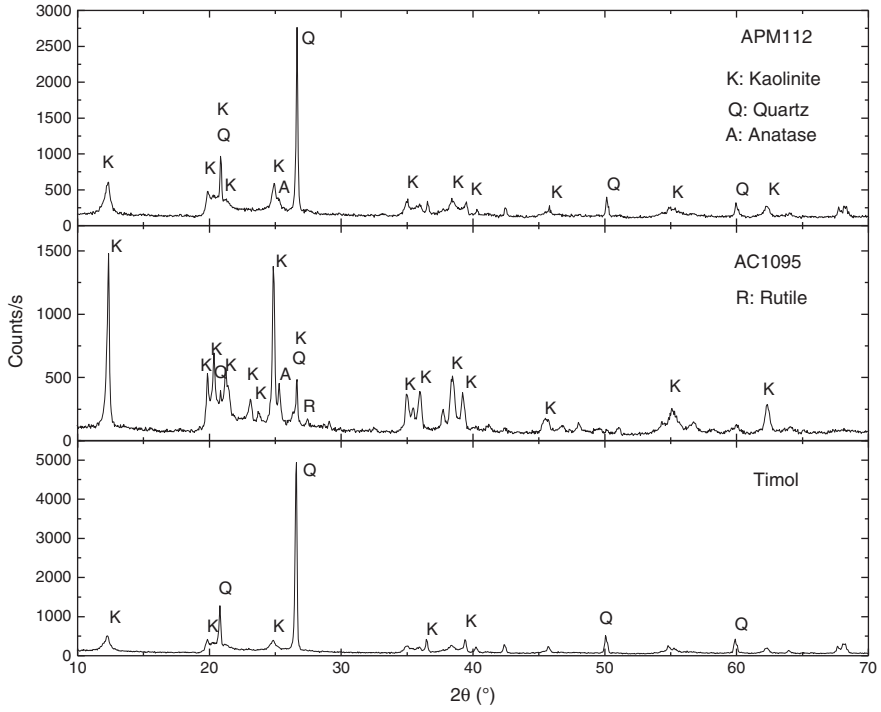

Fig. 1. Diffractograms of the three studied samples of refractory clays.

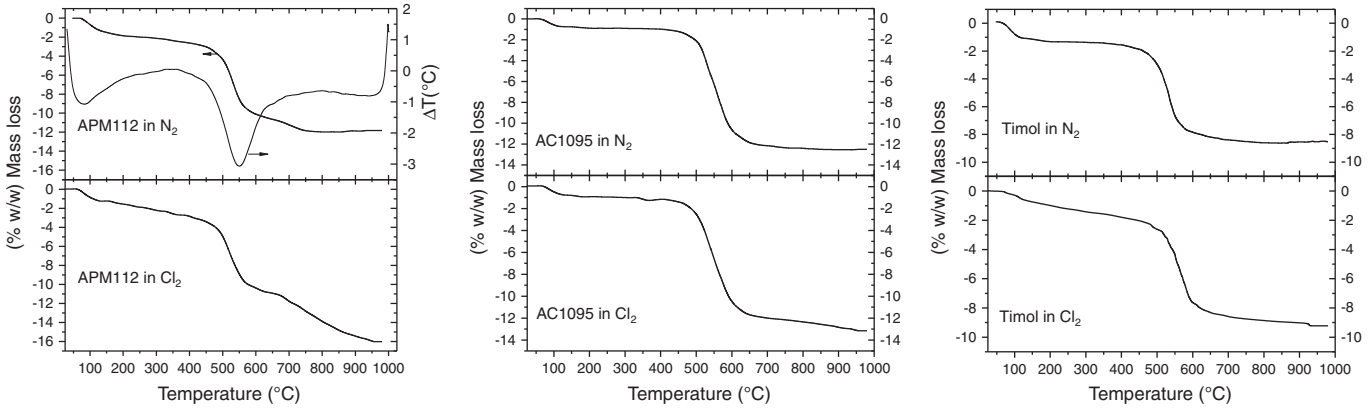

Fig. 2. Non isothermal thermogravimetry in N_2 and Cl_2/N_2 atmospheres.

control and early detection devices to identify possible gas leaks are currently available.

The thermodynamic analysis of the chlorination of iron present in refractory clays was carried out using the software HSC Chemistry for Windows 5.1 (HSC, 2003). According to the following data:

$$Fe_2O_3 + 3Cl_2(g) \rightarrow 2FeCl_3(g) + 1.5O_2(g) \quad (1)$$
$$\Delta G^\circ = (-0.049(T) + 59.5)\ (\text{kcal / mol of } Fe_2O_3)$$

and other associated minerals from different clays has been carried out without affecting their general composition. The effect of the organic matter present in clays and the optimal conditions of iron removal were established.

The purpose of this work was to carry out a thermogravimetric study of the chlorination of three different refractory clays samples used in the refractory materials industry in order to establish the optimal temperature range that allows quantitative removal of iron from this type of clay.

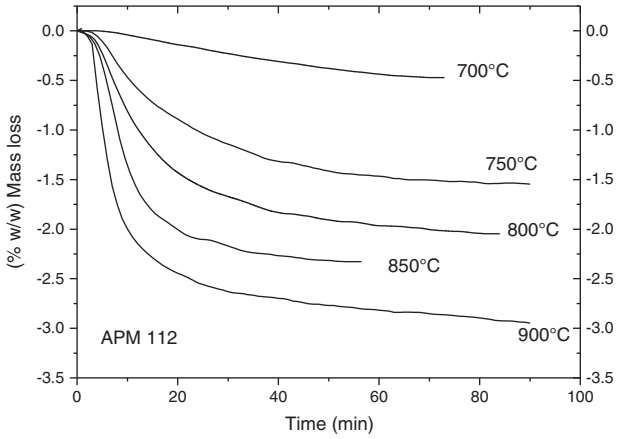

Fig. 3. Isothermal thermogravimetry in Cl_2/N_2 atmosphere.

Table 2
Analysis of Fe in the isothermal assays residues (%w/w).

Temperature (°C)	Fe_2O_3 in the residue	Fe extraction
700	2.6	25
750	1.9	46
800	1.1	69
850	0.9	74
900	0.5	86

2. Materials and methods

2.1. Materials

Three different samples were used in this investigation: APM112, AC1095 and Timol. The gases employed in the different assays were chlorine 99.5% (Indupa, Argentina) and nitrogen 99.99% (AGA, Argentina).

2.2. Equipment

The experimental chlorination assays, carried out with small amounts of mass, were performed in a thermogravimetric system designed in our laboratory (Túnez et al., 2007). The system was provided with a temperature programmer, flow meters and the acquisition of automatic data. The device was able to work with a mass of up to 0.5 g, with a sensitivity of 0.1 mg.

In order to obtain samples for the residues characterization, the calcination assays in N_2 and Cl_2/N_2 were carried out with higher amounts of mass. They were performed in a quartz tubular reactor with fluid dynamic conditions, similar to the thermogravimetric system. Consequently, the results obtained in both equipments might be compared and correlated.

The chemical composition of the samples and the iron content of the residues from the different treatments were obtained by X-ray fluorescence (XRF) with a Philips PW 1400 equipment. The analysis by X-ray diffraction (XRD) was carried out with a Rigaku D-Max-IIIC equipment, Cu–Kα, operated at 35 kV, 30 mA, and the BET surface area analysis was performed with a Micromeritics Gemini V equipment. The characterizations by scanning electron microscopy (SEM) and electron probe microanalysis (EPMA) were obtained using a LEO 1450VP microscope coupled to a Genesis 2000 EDS spectrometer. The colorimetric analysis was carried out with a MiniScan EZ spectrophotometer.

3. Procedure

The assays in the thermogravimetric system were carried out using masses of approximately 300 mg of powder sample, without previous treatment. For the thermal treatment, flows of 50 ml/min of N_2 and 50 ml/min of Cl_2/N_2 (50%) were used in an inert and in a chlorine gas environment, respectively. A linear heating program of 5°/min until the final programmed temperature was used for the non-isothermal assays. In the isothermal experiments, the sample was heated in an N_2 current (5°/min) until the programmed temperature was reached, and a flow of Cl_2/N_2 (50%) was introduced during the fixed time.

For the experimental studies carried out with the quartz tubular reactor, 2 g of sample without previous treatment and flows of 100 ml/min of N_2 and 100 ml/min of Cl_2/N_2 (50%) were used in an inert and a chlorine gas environment, respectively. The heating program of 5°/min was used to reach the final programmed temperature, and the sample was kept at this temperature for two hours.

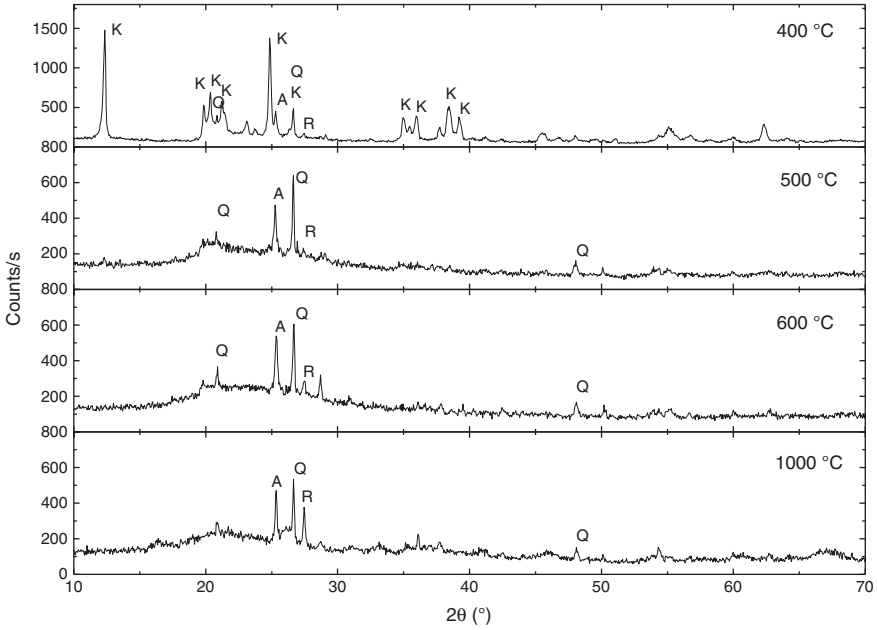

Fig. 4. Diffractograms of the AC1095 sample calcinated in N_2.

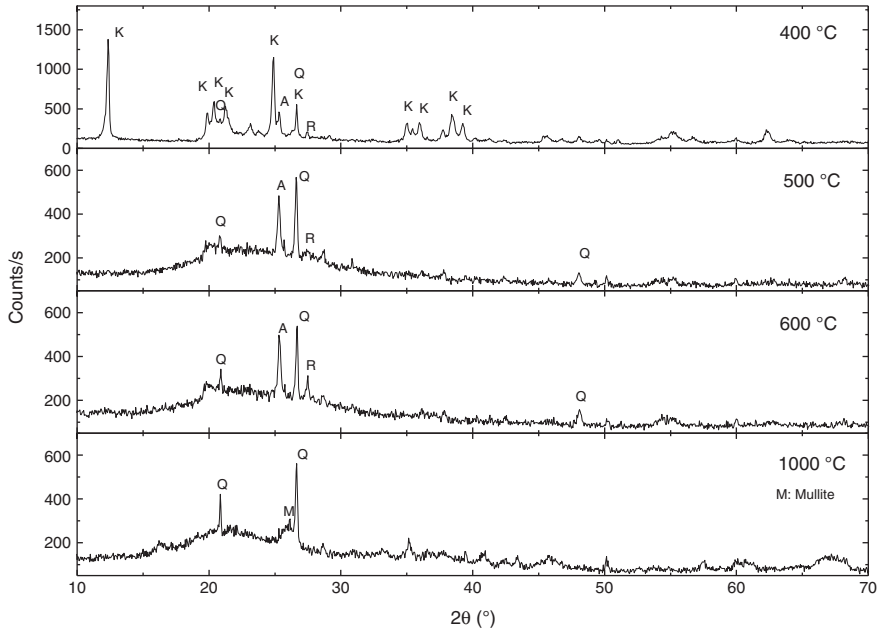

Fig. 5. Diffractograms of the AC1095 clay sample calcinated in a current of Cl_2/N_2.

4. Results and discussion

4.1. Samples characterization

The results of the analyses of the three samples using XRF are shown in Table 1. The AC1095 sample had a high content of Al_2O_3 and the least quantity of Fe_2O_3 whereas the APM112 sample had the least purity with a low content of Al_2O_3 and 3.5% of Fe_2O_3.

The diffractograms of minerals (Fig. 1) indicated that these samples contained kaolinite as clay mineral and quartz, anatase and rutile as associated minerals. The comparisons between the intensity of reflections corresponding to each mineral showed that the AC1095 sample had the least quantity of quartz while the Timol had the highest content. These results were in agreement with the chemical composition (Table 1).

4.2. Non isothermal thermogravimetry in N_2 and Cl_2/N_2

The results of the thermal treatments of the samples in N_2 and Cl_2/N_2 flows, using the thermogravimetric system, are shown in Fig. 2.

The calcination curves of the three samples in N_2 showed a first mass loss of about 2% between room temperature and 200 °C, which corresponded to the hydration water of samples. Between 450 °C and 650 °C, a second mass loss was observed in the three samples due to the transformation of kaolinite into metakaolinite. For the calcination of sample AC1095 in N_2, the analysis by DTA has been included in Fig. 2a, in which two endothermic regions corresponding to the loss of the hydration water and to the transformation of kaolinite into metakaolinite are observed. At high temperatures, an exothermic peak corresponding to the crystallization of mullite is observed. Similar results were obtained for clays APM112 and Timol. The obtained experimental data are in agreement with previous reports on this type of clays (Chakraborty, 2003; Castelein et al., 2001; Chen et al., 2004).

The APM112 sample exhibited a third light mass loss at temperatures higher than 650 °C, which may be attributed to the presence of a different type of clay mineral undetected by XRD, or to associated phases of aluminium and iron hydrated oxides. The mass loss attributed to the transformation of kaolinite into metakaolinite was higher in the AC1095 sample and lower in the Timol. This fact was

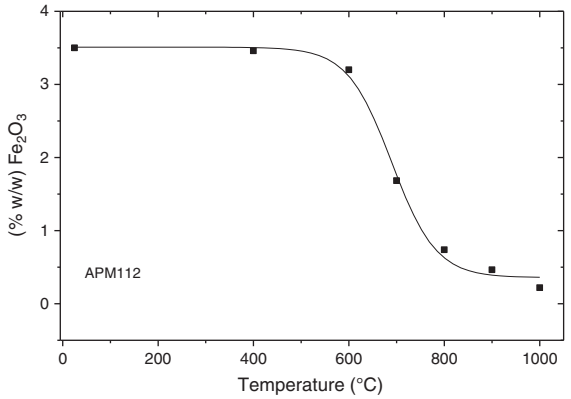

Fig. 6. Contents of Fe_2O_3 in the chlorination residues at different temperatures, determined by XRF.

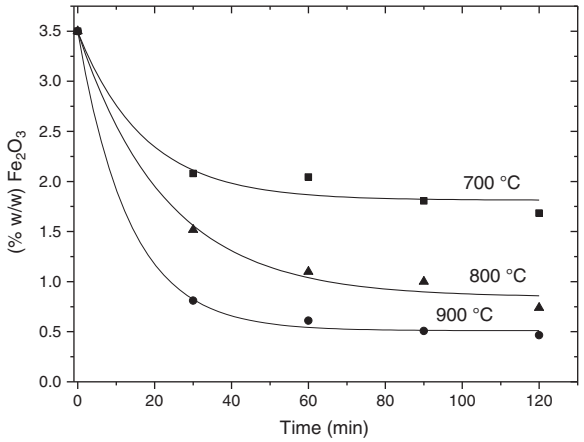

Fig. 7. Contents of Fe_2O_3 obtained at different times for the chlorination isotherms of APM112 sample.

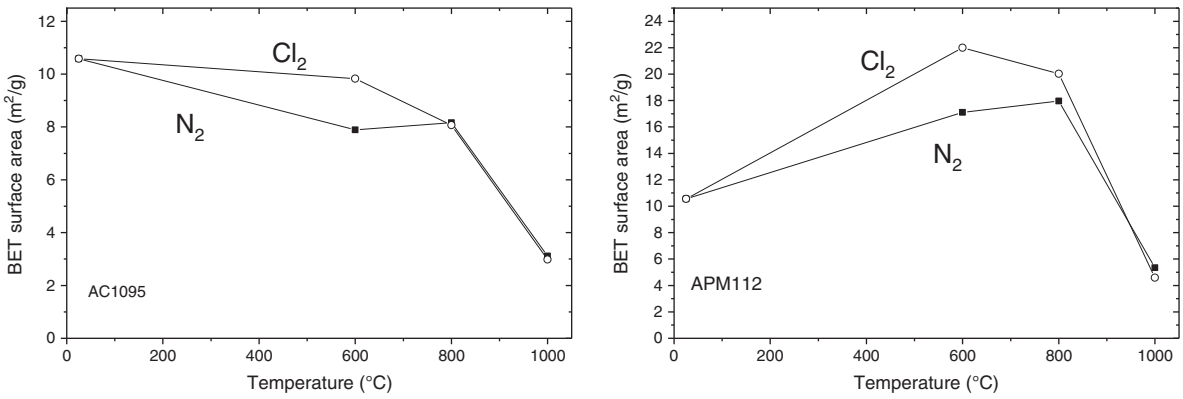

Fig. 8. Specific surface area of the untreated samples and of the calcination residues in N_2 and N_2/Cl_2.

in agreement with the chemical composition and the XRD analysis (Table 1 and Fig. 1).

When the samples were calcinated, the iron concentration in the sample increased due to a factor proportional to the previously mentioned mass loss. During the treatment at high temperatures in N_2, a mass loss involving iron compound volatilization was not observed. Consequently, for the analysis of Fe in the different residues, a sample calcinated in N_2 under conditions identical to the current assay was used as a reference pattern. The content of Fe was calculated in relation to the original content of Fe_2O_3 in the sample, independently from the crystalline structures in which this element was found in the sample (hydrated oxides, inferior oxidation states, or intra crystalline iron in kaolinite).

The comparison between the thermogravimetric curves until 750 °C in Cl_2/N_2 and those obtained in N_2 did not show significant changes in relation to the mass loss values and the temperatures at which transformations were produced. However, a significant difference was observed between both treatments at temperatures higher than 750 °C. The mass losses due to the action of Cl_2 at a high temperature were of about 1%, 1.5% and 4% for the AC1095, Timol and APM112 samples, respectively. This fact was caused by reaction (1) of the different crystalline or amorphous species in which iron may appear after the thermal treatment.

4.3. Isothermal thermogravimetry in N_2 and Cl_2/N_2

The isothermal chlorination in N_2 and Cl_2/N_2 was carried out with the APM112 sample in order to observe the action of chlorine on the impurities at high temperatures. The AC1095 sample was used to study the transformation of phases due to its highest purity.

For the isothermal study between 700 and 900 °C, in the thermogravimetric system, the sample was taken to the desired temperature in a current of pure N_2. The sample was kept at that temperature until a constant mass value was obtained. Under these experimental conditions, the sample exhibited the mass losses observed in Fig. 2, the elimination of the hydration water and the transformation of kaolinite into metakaolinite. Then, this sample was chlorinated with Cl_2/N_2, and the mass loss versus time was recorded. The results are shown in Fig. 3.

Table 3
Color analysis of the APM112 sample in N_2 and Cl_2/N_2.

Temperature (°C)	a*		b*		L*	
	N_2	Cl_2	N_2	Cl_2	N_2	Cl_2
400	17.2	19.0	17.2	19.3	64.5	64.8
600	21.6	19.0	19.4	20.5	65.3	72.7
800	18.9	-1.3	17.0	10.0	69.5	98.1
1000	9.9	0.1	18.4	0.2	75.4	99.7

The comparison between Figs. 2 and 3 indicates that during the calcination in a current of Cl_2/N_2 at temperatures higher than 750 °C, the mass losses observed (Fig. 3) are due to the elimination of iron through reaction (1).

In order to determine if the observed mass losses were related to the removal of the iron, the quantitative analysis of Fe in the residues was carried out using XRF. The results are shown in Table 2.

The iron content in the residues was quite close to that estimated by the mass loss (Table 2). This fact showed that in the studied temperature interval only the iron was attacked. These results permitted to infer that a high removal of the iron present in refractory clays might be obtained by chlorination at 900 °C during a period of 90 min.

4.4. Thermal treatments in the tubular reactor

The thermal treatments in the tubular reactor were performed using the APM112 and AC1095 samples. The extraction of Fe was quantified on the APM112 sample while an analysis of the phases transformation produced by the thermal treatment was carried out on the AC1095 sample.

The diffractograms of the AC1095 sample after the thermal treatment in N_2 (Fig. 4) showed that at 400 °C no transformation of the kaolinite phase was observed while at 500 °C, the transformation of this phase was complete.

These results were in agreement with the non isothermal gravimetric results. Besides, in the studied temperature interval, there was no phase transformation of quartz whereas at 1000 °C a partial transformation of anatase into rutile was observed.

The results of the thermal treatment in Cl_2/N_2 are shown in Fig. 5.

The comparison between Figs. 4 and 5 indicated that the calcination effect on the samples in N_2 and Cl_2/N_2 was identical at 400° and 500 °C. The XRD analysis of the residue of chlorination at 1000 °C showed the presence of a light peak reflection corresponding to the mullite phase, and the disappearance of the anatase and rutile phases was also observed.

The content of Fe remaining in the residues after the thermal treatments in a Cl_2/N_2 (Fig. 6) indicated that the removal of iron started at 600 °C, and the rate of this process rapidly increased up to 900 °C. These results were in agreement with those shown in Fig. 2 and with those reported by other authors who studied hematite chlorination (Gennari and Pasquevich, 1996; Gennari et al., 1997; Kanari et al., 2010).

Considering the results of Fig. 6, three isothermal chlorination assays of the APM1095 sample were carried out in the tubular reactor at 700, 800 and 900 °C, and then, the iron content for each point of the isotherms was analyzed. The results (Fig. 7) showed a phenomenon similar to that observed in the thermogravimetric system (Fig. 3): a

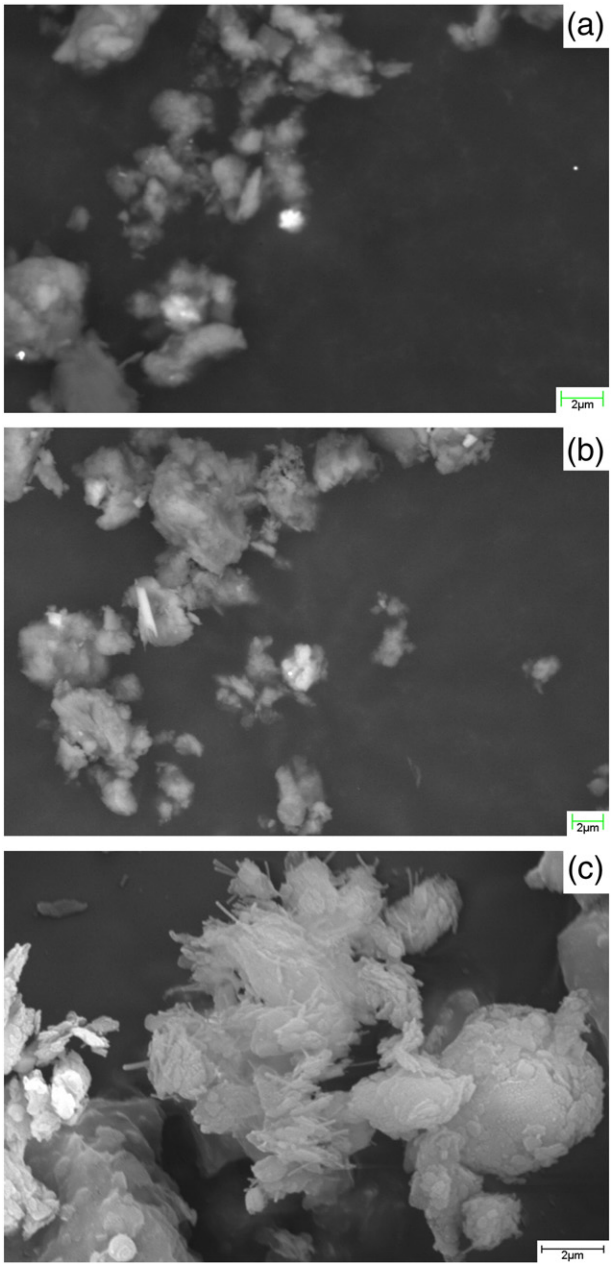

Fig. 9. SEM micrographs of the APM112 sample: (a) and (b) untreated; (c) calcinated in Cl_2/N_2.

rapid initial attack until about 60 min and a subsequent slow attack of Cl_2 gas on the sample.

A visual color exam of the residues from different temperatures indicated that under the experimental conditions the discoloration of the entire sample mass was homogeneous.

The determination of the BET surface area was carried out on the initial AC1095 and APM112 samples and on the residues of their respective calcinations in N_2 and Cl_2/N_2 at 600, 800 and 1000 °C. The results (Fig. 8) indicated that the APM112 and AC1095 samples had a similar initial specific surface area, and this area increased with the calcination temperature in N_2 until 800 °C for the APM112 sample. This area slightly decreased in AC1095 sample at the same temperature interval.

The thermal treatment of the APM112 sample in Cl_2/N_2 produced an increase of the specific surface area slightly higher than that observed in N_2. Between 600 and 800 °C, the specific surface area decreased in relation to that observed in N_2 due to the chlorine reaction with the sample.

The calcination of the AC1095 sample in Cl_2/N_2 up to 600 °C did not produce notable changes in the mineral specific surface area; from that temperature onwards a decrease was observed due to the mineral chlorination.

After the treatment at 1000 °C in both environments, the specific surface area of both samples decreased as a result of the beginning of the sintering process.

The reddish color of clays after calcination, according to the treatment received, indicated the presence of colloidal iron dispersed among the particles. To study this fact, a colorimetric analysis of the color space L*a*b* (also called CIELAB) was carried out. The results of the APM112 sample calcinated in N_2 and Cl_2/N_2 are shown in Table 3.

These data indicated that the parameters of color a* and b* decreased by chlorine action at a high temperature due to clay deferrification. The values of L* parameter indicated a notable increase of the clarity by this fact.

The SEM images of the untreated APM112 sample obtained with back-scattered electrons (Fig. 9a and b) permitted to observe brilliant particles. The micrograph of the residue corresponding to the chlorination of the APM112 sample at 1000 °C (Fig. 9c) showed the presence of small needle-shaped crystals and the disappearance of brilliant particles. The needle-shaped particles had a good correspondence with the mullite structures.

The EPMA analysis of these samples shown in Table 4 indicated that the brighter particles corresponded to a mineral with high iron content. The needle-shaped particles had a chemical composition similar to metakaolinite. This fact may be the result of the beginning of the mullite phase formation, detected by XRD, and the formation of vitreous silica. Similar phenomena were observed by González et al. (2007) when they studied the phase transformations in clays and kaolins produced by the thermal treatment in chlorine and air atmospheres.

5. Conclusions

The results of the chlorination study of the refractory clays obtained in the thermogravimetric system and in the quartz tubular reactor were coincident. In both cases, the chlorination reaction of the iron present in the samples started at around 700 °C and was completed at 900 °C. The results of the isothermal studies showed that the iron chlorination reaction was fast on the first 60 min, and then it was very slow. This phenomenon may be related to the different forms in which iron is found in clays, some of them requiring more energy for the element to be removed.

Chlorination has proved to be an efficient technique in the purification process of refractory clays. The chlorination using a mixture of Cl_2/N_2 at 50% at 800 °C for 2 h or at 900 °C for 30 min permitted a quantitative extraction of the iron present in the refractory clays. Under these working conditions, sintering was not produced, which may hinder the access of Cl_2 to the iron in the form of different compounds.

The extraction with Cl_2 of the iron present in the refractory clays was obtained without affecting the normal phases transformations suffered by these minerals due to the thermal treatment effect.

Table 4
EPMA analysis of the untreated APM112 sample and residue at 1000 °C (%w/w).

Sample	O	Al	Si	Fe
Brilliant particles, Fig. 9(a)	37.82	5.56	6.35	50.27
Brilliant particles, Fig. 9(b)	38.44	4.85	5.19	51.52
Small needle, Fig. 9(c)	57.84	19.37	21.65	1.14

The quantity of colloidal iron in the samples may be estimated on the basis of the red color parameters and the clarity. Although this datum did not permit to compare the iron content between different clays, the analysis of the data in Table 3 and Fig. 4 indicated that there was a good correspondence between the parameter color + a^* and that of clarity L^* with the iron content in the APM112 sample.

The analysis using SEM and EPMA indicated that the iron was found finely dispersed on the laminar particles of the clays and also forming small grains, and that this element was removed by the chlorine effect at high temperatures.

Acknowledgments

The authors wish to thank *Universidad Nacional de San Luis (UNSL)*, *Fondo Nacional para la Investigación Científica y Tecnológica (FONCyT)* and *Consejo Nacional de Investigaciones Científicas y Técnicas (CONICET)* for financial support. The SEM and EPMA studies were carried out in the *Laboratorio de Microscopía Electrónica y Microanálisis (LABMEM), UNSL.*

References

Ambikadevi, V.R., Lalithambika, M., 2000. Effect of organic acids on ferric iron removal from iron-stained kaolinite. Appl. Clay Sci. 16, 133–145.
Atkinson, M.L. Fleming, M.E., 2001. Methods for bleaching kaolin clay and other minerals and bleached products obtained by the method, EP Pat.1146089.
Bergaya, F., Theng, B.K.G., Lagaly, G., 2006. Handbook of Clay Science, Vol. 1. Developments in Clay Science.
Blumenthal, G., Wegner, G., 1989. Preferential formation of aluminium chloride by chlorination of a highly reactive powder obtained from metakaolin or kaolin by hydrochloric acid treatment. React. Solids 7 (2), 105–113.
Castelein, O., Soulestin, B., Bonnet, J.P., Blanchart, P., 2001. The influence of heating rate on the thermal behaviour and mullite formation from a kaolin raw material. Ceram. Int. 27, 517–522.
Chakraborty, A.K., 2003. DTA study of preheated kaolinite in the mullite formation region. Thermochim. Acta 398, 203–209.
Chandrasekhar, S., Ramaswamy, S., 2002. Influence of mineral impurities on the properties of kaolin and its thermally treated products. Appl. Clay Sci. 21, 133–142.
Chandrasekhar, S., Ramaswamy, S., 2006. Iron minerals and their influence on the optical properties of two Indian kaolins. Appl. Clay Sci. 33, 269–277.
Chen, Y., Moo-Chin, W., Min-Hsiung, H., 2004. Phase transformation and growth of mullite in kaolin ceramics. J. Eur. Ceram. Soc. 24, 2389–2397.
De Mesquita, L.M.S., Rodrigues, T., Gomes, S.S., 1996. Bleaching of Brazilian kaolins using organic acids and fermented medium. Miner. Eng. 9 (9), 965–971.
Fabry, C., Kleindl. F.K., 2001. Processes for producing a bleaching clay product. US Pat. 6288003.
Gennari, F.C., Pasquevich, D.M., 1996. Kinetics of chlorination of hematite. Thermochim. Acta 284, 325–339.
Gennari, F.C., Bohé, A.E., Pasquevich, D.M., 1997. Effect of reaction temperature on the chlorination of a Fe_2O_3–TiO_2–C mixture. Thermochim. Acta 302, 53–61.
González, J.A., Ruiz, M. del C., 2006. Bleaching of kaolins and clays by chlorination of iron and titanium. Appl. Clay Sci. 33, 219–229.
González, J.A., Carreras, A.C., Ruiz, M. del C., 2007. Phase transformations in clays and kaolins produced by thermal treatment in chlorine and air atmospheres. Lat. Am. App. Res. 37 (2), 133–139.
Habashi, F., 1986. Principles of Extractive Metallurgy. : Pyrometallurgy, Vol. 3. Gordon and Breach Science Publisher.
HSC, 2003. Chemistry for Windows Software V. 5.1. Outokumpu Research, Pori, Finland.
Jena, P.K., Brocchi, E.A., 1997. Metal extraction through chlorine metallurgy. Miner. Process. Extr. Metall. Rev. 16, 211–247.
Kanari, N., Mishra, D., Filippov, L., Diot, F., Mochón, J., Allain, E., 2010. Kinetics of hematite chlorination with Cl_2 and $Cl_2 + O_2$: part I. Chlorination with Cl_2. Thermochim. Acta 497 (1–2), 52–59.
Landsberg, A., 1975. Chlorination kinetics of aluminum bearing minerals. Metall. Trans. B 6B (2), 207–214.
Maurya, C.B., Dixit, S.G., 1990. Effect of pH on the High-gradient magnetic separation of kaolin clays. Int. J. Miner. Process. 28 (3–4), 199–207.
Raghavan, P., Chandrasekhar, S., Damodaran, A.D., 1997. Value addition of paper coating grade kaolins by the removal of ultrafine coloring impurities. Int. J. Miner. Process. 50, 307–316.
Roder, Zs., Bertóti, I., Székely, T., 1987. Reaction of metakaolinite with phosgene and carbon tetrachloride. React. Solids 3 (1–2), 113–125.
Túnez, F. M., González, J. y Ruiz, M. del C., 2007. Aparato de Laboratorio para Realizar Termogravimetrías en Atmósferas Corrosivas y no Corrosivas, AR Pat. 053676.
Veglio', F., Toro, L., 1994. Process development of kaolin pressure bleaching using carbohydrates in acid media. Int. J. Miner. Process. 41 (3–4), 239–255.